Schwank, M., Guglielmetti, M., Mätzler, C., Oberdörster, C., Vanderborght, J., Flühler, H. (2008): FOSMEX: Forest Soil Moisture Experiments with Microwave Radiometry. - IEEE Transactions on Geoscience and Remote Sensing, 46, 3, 727-735

DOI: 10.1109/TGRS.2007.914797

FOSMEX: Forest Soil Moisture Experiments With Microwave Radiometry

Massimo Guglielmetti, Mike Schwank, Christian Mätzler, *Senior Member, IEEE*, Christoph Oberdörster, Jan Vanderborght, and Hannes Flühler

***Abstract*—The microwave Forest Soil Moisture Experiment (FOSMEX) was performed at a deciduous forest site at the Research Centre Jülich (Germany). An L- and an X-band radiometer were mounted 100 m above ground and directed to the canopy. The measurements consist of dual- and single-polarized L- and X-band data and simultaneously recorded ground moisture, temperature, and meteorological data. The canopy L-band transmissivity was estimated from a subset of the FOSMEX data, where the ground was masked with a metalized foil. For the foliage-free canopy, the reflecting foil diminished the L-band brightness by ≈24 K, whereas brightness increased by ≈14 K when the foil was removed from below the foliated canopy. Depending on the assumption made on the scattering albedo of the canopy, the transmissivities were between 0.2 and 0.51. Furthermore, the contribution of the foliage was quantified. Although, the evaluation revealed the semitransparency of the canopy for L-band frequencies, the brightness sensitivity with respect to ground moisture was substantially reduced for all foliation states. The effect of ground surface moisture was explored in an irrigation experiment. The L-band measurements were only affected for a few hours until the water drained through the litter layer. This emphasizes the significance of the presence of litter for soil moisture retrieval from remotely sensed L-band brightness data. The FOSMEX database serves for further testing and improving radiative transfer models used for interpreting microwave data received from future spaceborne L-band radiometers flying over areas comprising a considerable fraction of deciduous forests.**

***Index Terms*—Canopy transmissivity, forest, microwave radiometry, radiative transfer, soil moisture.**

I. Introduction

AREAL soil water content is a key variable for estimating water and energy fluxes at the Earth's surface, in particular, the actual evapotranspiration [1]. Passive microwave radiometry at L-band (1–2 GHz) was demonstrated to be most suitable for soil water detection on large scales [2]–[5], mainly because of the relatively deep emission depth compared to measurements at shorter wavelengths [6], [7] and because of its ability to penetrate vegetation covers [8].

One of the objectives of the upcoming Soil Moisture and Ocean Salinity mission (SMOS) is monitoring the Earth's surface moisture with a full coverage of the globe in three days and at a spatial resolution of approximately 40×40 km^2 [5]. In most instances, the observed footprint includes different landscape elements ranging from bare soils to terrains covered with various vegetation types (grasses, bushes, crops, forests, etc.). Consequently, knowing the radiation signatures of the most abundant and important landscape units is essential for correctly interpreting the brightness signal, which is a composite of subgrid footprint information. Forested terrain constitutes approximately one third of the Earth's land surface, excluding Antarctica and Greenland, and is therefore a quantitatively relevant landscape element.

Discrete radiative transfer approaches used for forward modeling the L-band radiation of forests are presented in [9]–[11]. These sophisticated approaches are using dielectric cylinders with known radiation patterns, suitably arranged for representing the morphology of a forest stand and the corresponding forest radiation. For low microwave frequencies, the forest canopies are predicted to be semitransparent, which allows measurements of the radiation emitted from below the canopy. The contributions of the tree components with respect to the total forest radiation were modeled. It was found that branches are the most relevant tree components with respect to L-band radiation, whereas trunks, leaves, or needles are less important. On the basis of allometric equations, a realistic description of the forest canopy structure was proposed in [12] and [13] and combined with a discrete radiative transfer approach for modeling the L-band emission of coniferous forests [11].

Despite of the high relevance of forest canopies for interpreting the upcoming SMOS data, the experimental knowledge on L-band radiation measured above forests is limited and controversial. The microwave emission from a forested area measured from a satellite is reported in [14]. Results from airborne measurements are shown in [8] and [15], and results of a tower-based study are presented in [16]. A multifrequency passive microwave experiment performed from below a single beach tree is discussed in [17]. A detailed summary of important experimental and theoretical investigations related to the microwave emission of forests at regional and global scale can be found in [18].

Manuscript received February 26, 2007; revised August 17, 2007. This work was supported in part by the Swiss Federal Institute of Technology (Eidgenoessische Technische Hochschule (ETH) Zurich) and in part by the German Research Foundation (DFG) funded project "Combining remote sensing and geophysical methods for monitoring and modeling of water fluxes and soil water dynamics in a forest stand."

M. Guglielmetti and H. Flühler are with the Institute of Terrestrial Ecosystems, Swiss Federal Institute of Technology Zürich, 8092 Zürich, Switzerland (e-mail: massimo.guglielmetti@env.ethz.ch; fluehler@env.ethz.ch).

M. Schwank is with the Swiss Federal Institute for Forest, Snow and Landscape Research, 8903 Birmensdorf, Switzerland (e-mail: mike.schwank@wsl.ch).

C. Mätzler is with the Institute of Applied Physics, University of Bern, 3012 Bern, Switzerland (e-mail: christian.matzler@mw.iap.unibe.ch).

C. Oberdörster and J. Vanderborght are with the Agrosphere Institute, Institute of Chemistry and Dynamics of the Geosphere (ICG-4), Forschungszentrum Jülich GmbH, 52428 Jülich, Germany (e-mail: c.oberdoerster@fz-juelich.de; j.vanderborght@fz-juelich.de).

Digital Object Identifier 10.1109/TGRS.2007.914797

In an earlier campaign performed during fall of 2004 at the same site as the Forest Soil Moisture Experiment (FOSMEX) presented hereafter, the downwelling L- and X-band radiation was measured from below the forest canopy [19]. L-band transmissivities for the foliated and the foliage-free canopy were found to be 0.41 to 0.46, revealing the semitransparency and the minor impact of foliation. The X-band canopy transmissivity was significantly lower at the foliated state, and the sensitivity to the presence of leaves was clearly higher.

To our knowledge, there is a lack of studies in which the feasibility of forest soil moisture retrieval on the basis of measured L-band brightness temperatures is experimentally tested. This and the need for validating the radiative transfer model to be used for interpreting SMOS data were the motivation for conducting the FOSMEX campaign.

An L- and an X-band RadioMeter (RM) mounted on a tower above a deciduous forest site were used in the FOSMEX. Forest ground temperature and permittivity, which were correlated with moisture [20], were measured simultaneously with the remotely sensed RM data. The experiment was run under natural meteorological conditions and under the following two experimentally modified conditions: 1) The forest ground was masked (foil experiment) and 2) irrigated (irrigation experiment). The conducted FOSMEX campaign provides a one-year data set relating L-band brightness emitted from the forested site with physical temperatures and canopy foliation state. The presence of litter is identified to be important, as the emissivity of the forest ground is highly affected by the impedance match between the air and bulk soil caused by the intermediate litter layer. The presented experimental results provide key information for the L-band Microwave Emission of the Biosphere (L-MEB) model designated to be used in the SMOS level-2 algorithm [21].

II. Field Experiment

FOSMEX was performed from January 10, 2005 (= Day of Year (DoY) 10) to January 9, 2006 (= DoY 9). An L- and an X-band RM have been deployed above a mature deciduous forest located at the Research Centre Jülich (Germany). Section II-A describes the experimental setup of the one-year campaign. Basic characteristics of the deployed microwave RMs are given in Section II-B, and the relevant forest canopy parameters and meteorological conditions at the site are reported in Section II-C. The setups of the foil and irrigation experiment performed during the FOSMEX campaign are described in Sections II-D and E.

A. Experimental Setup

The 1.4-GHz and the 11.4-GHz RMs ELBARA and MORA were deployed on the 100-m-high platform of the meteorological tower located within the forest stand (Fig. 1). An automated elevation positioner was used, allowing for detecting radiances at angles between $45^\circ \leq \alpha \leq 70^\circ$ relative to the vertical direction. The scanning positioner is driven with a stepping motor and a worm gear with a high reduction [19]. A Campbell datalogger CR10X was used for controlling purposes.

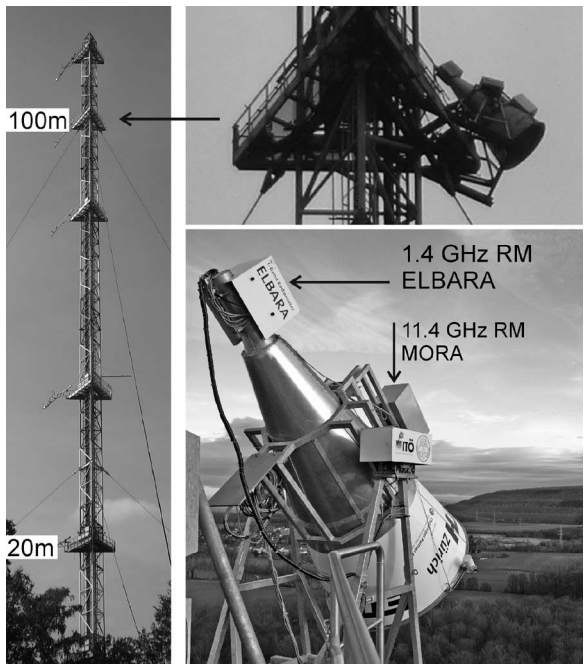

Fig. 1. Meteorological tower and RMs mounted on the 100-m platform of the meteorological tower located within a deciduous forest stand at the Research Centre Jülich (Germany).

Air temperature and precipitation were detected on the tower platform at 20-m height. Forest ground temperatures were measured *in situ* with thermistors (Campbell S-TL107) at 5-cm depth. Time series of soil permittivities (real parts) at frequencies < 2 GHz were measured with Time Domain Reflector (TDR) probes installed 5 cm below the litter layer mainly consisting of dead leaves. These data, as well as the microwave brightness data, were stored on a Campbell CR10X datalogger. Two digital optical cameras were installed below and above the canopy to record the temporal evolution of the canopy in terms of its foliation state.

The time resolution of the simultaneously measured ground-truth and RM data was mostly 2 h. However, during three days of the irrigation experiment, it was increased to 5 min. The meteorological data were recorded hourly and averaged over 2 h during the entire campaign.

B. Remote Sensing System

The L- and X-band RMs ELBARA and MORA operate at the center frequencies of $f = 1.4$ and 11.4 GHz, corresponding to the vacuum wavelengths $\lambda \approx 21$ and 2.6 cm. A detailed technical description of ELBARA and MORA can be found in [22] and [23].

ELBARA is a Dicke-type RM, allowing for measuring at horizontal (H) and vertical (V) polarization. Radiances of internal cold (278 K) and hot (338 K) loads are measured for calibration before measuring the brightness temperature of the scene. The absolute accuracy and sensitivity of brightness measured with ELBARA under laboratory conditions for the temperature range of 238–338 K were determined to be better than ± 1 K and < 0.1 K, respectively [22]. To distinguish manmade from natural noise, the brightness is split into two channels as follows: one working between 1.400–1.418 GHz and the other

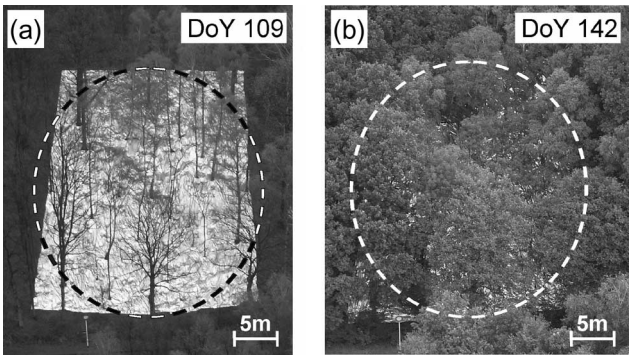

Fig. 2. Observed scene and (dashed lines) -3-dB footprint at $\alpha = 46^\circ$ during the foil experiment. (a) Foliage-free. (b) Foliated forest state.

between 1.409–1.427 GHz. Furthermore, the measurements are corrected for absorption occurring in the cables between the antenna and the RM front-end. MORA is also a Dicke-type RM operating at vertical polarization only. The calibration was carried out periodically using the sky radiance and a black-body source with known temperature.

Both RMs were equipped with conical horn antennas with -3-dB full beamwidth of 12° and symmetrical beams with small $(< -30\text{-dB})$ sidelobes [24]. The radiance received from the -3-dB footprint comprises approximately 50% of the total emission of the observed scene [25].

C. Field-Site Conditions

FOSMEX was performed above the deciduous mixed forest in Jülich (Germany), which is situated at longitude $50^\circ 50' 30$ N, latitude $6^\circ 21' 30$ E, and elevation 83 m above sea level. Total precipitation during the one-year campaign was 673 mm. The tree age was between 40 and 80 years, and the average crown height was approximately 24 m. The forest comprised of oak, birch, and beech in similar proportions. The ground area within the first 80 m from the tower (area below the zone shown in Fig. 2) was mainly woodless but overgrown with low shrubs.

The column density of the dry canopy biomass was estimated from the corresponding tree trunk diameters at breast height (1.4 m above ground) using the empirical model proposed in [26]. The canopy column density is estimated to be 15 kg m^{-2} within the forest area of approximately 1250 m^2 corresponding to the -3-dB footprint at the observation angle $\alpha = 46^\circ$ (see Section II-D). The maximal column density of the fresh leaves, for the fully foliated canopy state, was experimentally determined as 1.14 kg m^{-2} [19], and the volumetric and the gravimetric water content of the fresh bulk leaf material was approximately 0.5 m^3 m^{-3} and 0.5 kg^3 kg^{-3}, respectively.

The shooting of the leaves in spring 2005 started after mid-April and lasted for one month. Defoliation phase took place from mid-October to mid-November. The relative foliation was quantified by means of regularly taken photos.

Mean air temperature during the campaign measured on the tower platform at 20-m height was $\langle T_{\rm A} \rangle = 283.9$ K. The average forest ground temperature $\langle T_{\rm FG} \rangle = 283.6$ K was measured at 5-cm depth at 15 representative locations along two transects between trees. Time series of $T_{\rm A}$ (gray) and $T_{\rm FG}$ (black) during the one-year campaign are shown in Fig. 3(a).

D. Foil Experiment

For investigating the microwave transmissivity of the canopy, the area of the forest ground overlapping with the -3-dB footprint at observation angle $\alpha = 46^\circ$ was covered with a metalized plastic foil. The foil experiment was started before the shooting of the leaves [Fig. 2(a)] on DoY 109 (April 19) and ended on DoY 142 (May 22) when the forest was in its fully foliated state [Fig. 2(b)].

Before the foil was laid on the ground, the understory vegetation and dead branches were removed. Afterward, the foil was spread out as a rectangle of approximately 47×27 m^2. Pegs were used for fixing the 1.29-m-wide foil stripes on the ground in between the tree trunks. Furthermore, the stripes were taped together approximately every meter to prevent it from being blown away. As shown in Fig. 2, the elliptic -3-dB footprint (dashed lines) with an area of $\approx$1200 m^2 at $\alpha = 46^\circ$ is closely covered by the masked area.

The composite foil was made up of a 12-μm-thick aluminum film in between 12 μm of polyester and 75 μm of polyethylene. The thickness of the electrically conductive and paramagnetic aluminum is significantly larger than the skin depth at L- and X-band frequencies. Furthermore, the lateral dimension of the foil corrugation was larger than the Bragg limit ($\approx$15 cm $\approx$ resolution limit) at L-band, and the selected observation angle α [28, Sec. 4.7] yields to a highly reflecting surface, which shields the ground emission almost perfectly.

E. Irrigation Experiment

The same area which was covered with the foil was irrigated on DoY 277 (October 4) at 2 P.M. after a rainless period of five days. Furthermore, the rainless period continued for the following three days. During the irrigation experiment, the canopy was still fully foliated, and the -3-dB footprint at $\alpha = 46^\circ$ was still without understory vegetation as it has been removed for the preceding foil experiment.

The irrigation water was sprinkled onto the rectangular area $(47 \times 27$ m$^2)$ shown in Fig. 2(a) with hoses operated by five firemen. In 1 h, the volume of 60.2 m^3 of water at approximately ambient temperature was sprinkled as uniformly as possible, whereas wetting the tree canopy was avoided. The corresponding irrigation rate of 45.2 mm h^{-1} corresponds to a high-intensity rainfall. Hence, we expect that irrigation affects the microwave signature at least as much as a natural rainfall event.

Before and after the irrigation, forest ground permittivities $\varepsilon_{\rm FG}$ were measured within the irrigated area approximately 5 cm below the litter layer using eight TDR probes distributed within an area of 10×10 m^2. These measurements provided time series $\varepsilon_{\rm FG}$ of the bulk surface soil, but the temporal evolution of the litter layer permittivity remained unobserved.

III. Microwave Radiative Transfer Model

The brightness temperature $T_{\rm B}$ measured above a bare-soil site is the sum of the soil emission and the reflected sky brightness $T_{\rm B,sky}$ (cosmic background plus atmosphere).

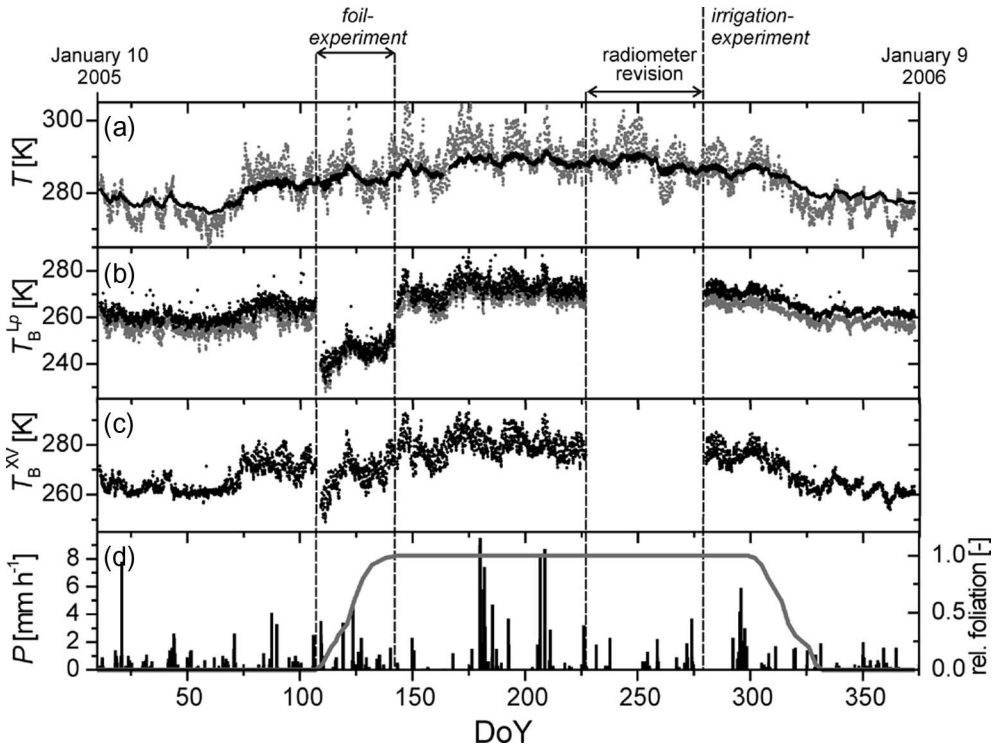

Fig. 3. FOSMEX data set. (a) (black) Forest ground temperature T_{FG} and (gray) air temperature T_{A}. (b) L-band brightness temperature $T_{\mathrm{B}}^{\mathrm{L}p}$ at polarization (gray) $p = \mathrm{H}$, (black) V. (c) X-band brightness temperature at V-polarization $T_{\mathrm{B}}^{\mathrm{XV}}$. (d) Average of 2 h of the (columns) precipitation P and relative foliation state of the (gray line) forest canopy.

However, in the presence of vegetation, the absorption and self-emission of the canopy has to be accounted for. In the FOSMEX, the situation is slightly more complex, as various areas with different effective site parameters are contributing to the measured brightness T_{B}. This requires T_{B} modeling as a linear combination of the partial radiances $T_{\mathrm{B},i}$ emitted by the K areas $i = 1, \ldots, K$ within the instrumental field of view

$$T_{\mathrm{B}} = \sum_{i=1}^{K} \mu_i T_{\mathrm{B},i}. \tag{1}$$

The fractional amount μ_i of which $T_{\mathrm{B},i}$ contributes to the total T_{B} is estimated from the antenna directivity integrated over the solid angle associated with the area i. The brightness $T_{\mathrm{B},i}$ is computed using the zeroth-order radiative transfer approach [27], which is also called τ–ω model [21]. Thereby, the wave propagation through the canopy is expressed by the effective single-scattering albedo ω_i and the transmissivity Γ_i. Mean forest ground and vegetation temperatures $T_{\mathrm{FG},i}$ and $T_{\mathrm{V},i}$, as well as the ground reflectivity $R_{\mathrm{FG},i}$, are used in the model

$$\begin{aligned} T_{\mathrm{B},i} = {} & T_{\mathrm{FG},i}(1 - R_{\mathrm{FG},i})\Gamma_i + T_{\mathrm{V},i}(1 - \Gamma_i)(1 - \omega_i) \\ & + T_{\mathrm{V},i}(1 - \Gamma_i)(1 - \omega_i) R_{\mathrm{FG},i}\Gamma_i \\ & + T_{\mathrm{B,sky}}\left[R_{\mathrm{FG},i}\Gamma_i^2 + \omega_i(1 - \Gamma_i)(1 + R_{\mathrm{FG},i}\Gamma_i)\right]. \end{aligned} \tag{2}$$

The four radiation contributions for $T_{\mathrm{B},i}$ are interpreted as follows: 1) forest ground emission propagated through the canopy; 2) vegetation emission in upward direction; 3) vegetation emission reflected at the ground and propagated through the canopy; and 4) sky radiance contribution. This model yields a lower bound for the brightness $T_{\mathrm{B},i}$. Furthermore, (2) fulfills Kirchhoff's law, as a proper sky term 4) is used (compare in [28, eq. (4.1), p. 228]).

For both the foil and irrigation experiment described in Sections II-D and E, three different areas $(K = 3)$ with corresponding radiation weights μ_1, μ_2, and μ_3 are relevant. The fraction $\mu_1 = 0.50$ associated with the radiation of the either masked or irrigated area [Fig. 2(a)] was estimated from the antenna directivity integrated over the -3-dB aperture angle. In analogy, the small fraction $\mu_2 = 0.07$ representing the radiation contribution of the mainly woodless zone closer than 80 m to the tower (area below the zone as shown in Fig. 2) was estimated. The remaining fraction $\mu_3 = 1 - \mu_1 - \mu_2 = 0.43$ is the radiation weight of the remaining forested area.

IV. Results and Discussion

Section IV-A gives a survey of the entire one-year FOSMEX data set consisting of microwave and meteorological data. Results deduced from the foil and the irrigation experiment performed within FOSMEX are presented in Sections IV-B and C.

A. FOSMEX Data Set

The meteorological and the microwave data measured during the entire campaign (365 days) are shown in Fig. 3. The campaign started on January 10, 2005 (DoY 10) and ended on January 9, 2006 (DoY 9). The period of the foil experiment ($109 \leq$ DoY ≤ 142, April 19–May 22) and the date of

the irrigation experiment (DoY 277, October 4) are shown in Fig. 3.

Temperatures $T_{\rm FG}$ (black) and $T_{\rm A}$ (gray) of the forest ground and the air are shown in Fig. 3(a); L-band brightness temperatures $T_{\rm B}^{{\rm L}p}$ at polarization $p = {\rm H}$ (gray), V (black) are shown in Fig. 3(b); X-band brightness $T_{\rm B}^{\rm XV}$ at vertical polarization are shown in Fig. 3(c); and the 2-h averages of precipitation P (columns) and the relative canopy foliation state (gray line) are presented in Fig. 3(d).

The radiometric data shown are restricted to the observation angle $\alpha = 46^\circ$ corresponding to the -3-dB footprint, as shown in Fig. 2. Furthermore, no radiometric measurements were taken between $227 \leq {\rm DoY} \leq 275$ due to technical problems with ELBARA. These instrumental problems were related to the cold load used for the internal calibration and to a gain-failure of one of the amplifiers along the microwave path. As a consequence, L-band brightness $T_{\rm B}^{{\rm L}p}$ measured before the RM revision (DoY $<$ 227) were calibrated using the sky-brightness $T_{\rm B,sky}$ diurnal measured at midnight and the hot load instead of using the device internal cold and hot load. The resulting absolute accuracy of $T_{\rm B}^{{\rm L}p}(p = {\rm H}, {\rm V})$ measured with ELBARA before repair was estimated to be ± 3 K, which is less accurate as compared with the performance of ELBARA in its nominal mode (better than ± 1 K).

The L- and X-band brightness temperatures $T_{\rm B}^{{\rm L}p}$ and $T_{\rm B}^{\rm XV}$, shown in Fig. 3(b) and (c), change synchronously with the thermodynamic temperatures $T_{\rm FG}$ and $T_{\rm A}$, as shown in Fig. 3(a). High values of scene emissivities > 0.85 (defined as the ratio between the brightness and the thermodynamic temperature) at both frequencies (1.4 and 11.4 GHz) and for any canopy state are observed. Comparable values of typical scene emissivities were found for a pine forest in Les Landes (France) [16].

The measured L-band brightness $T_{\rm B}^{\rm LV}$ (black) at vertical polarization generally exceed the values $T_{\rm B}^{\rm LH}$ (gray), which is observed at horizontal polarization $(T_{\rm B}^{\rm LV} > T_{\rm B}^{\rm LH})$. Consequently, the polarization ratio defined as $PR = 2(T_{\rm B}^{\rm LV} - T_{\rm B}^{\rm LH})/(T_{\rm B}^{\rm LV} + T_{\rm B}^{\rm LH})$ [29] is typically positive for the performed L-band measurements. The annual mean difference $\langle T_{\rm B}^{\rm LV} - T_{\rm B}^{\rm LH} \rangle = 3.5$ K $\pm$ 2.1 K (excluding the foil experiment and the revision period) is small, indicating that L-band brightness emitted from the forested area is vertically polarized to a minor degree. The slightly vertically polarized L-band radiation can be attributed to the radiation contribution of the vertically polarized ground emission propagated through the canopy [term 1) in (2)]. This can be constituted from the analysis of the polarization of the individual radiation contributions [terms 1)–4)] of the radiative transfer model (2). Since ground emissivities $(1 - R_{\rm FG}^p)$ are higher for the V- than for the H-polarization, the radiation emitted from the ground [term 1)] is vertically polarized. On the contrary, the remaining radiation contributions [terms 2)–4)] are horizontally polarized. This is either due to $R_{\rm FG}^{\rm H} > R_{\rm FG}^{\rm V}$ or due to the horizontally polarized canopy emission (implying that $1 - \Gamma^{\rm LH} > 1 - \Gamma^{\rm LV}$) found in the earlier campaign, where $T_{\rm B}^{\rm LV} - T_{\rm B}^{\rm LH} \approx -10$ K was observed in most cases [19].

Increasing differences $T_{\rm B}^{\rm XV} - T_{\rm B}^{\rm LV}$ between vertically polarized brightness temperatures measured at L- and at X-band were found for more developed foliation states. This is shown on account of measured mean differences during two foliage-free periods and a period of fully developed foliage. For the two foliage-free periods $10 \leq {\rm DoY} \leq 70$ and $345 \leq {\rm DoY} \leq 9$, one finds $\langle T_{\rm B}^{\rm XV} - T_{\rm B}^{\rm LV} \rangle = 2.9$ K $\pm$ 2.0 K and $\langle T_{\rm B}^{\rm XV} - T_{\rm B}^{\rm LV} \rangle = -0.8$ K $\pm$ 2.0 K, whereas the corresponding difference $\langle T_{\rm B}^{\rm XV} - T_{\rm B}^{\rm LV} \rangle = 7.0$ K $\pm$ 2.5 K found for the period $143 \leq {\rm DoY} \leq 226$ of maximum foliation is significantly higher. The observed rise of the difference $\langle T_{\rm B}^{\rm XV} - T_{\rm B}^{\rm LV} \rangle$ with increasing foliage is due to the higher canopy emission at X- than at L-band. This distinctly different influence of the foliation state on the X- and L-band radiation has already been observed in [19] and will be confirmed in the foil experiment (Section IV-B).

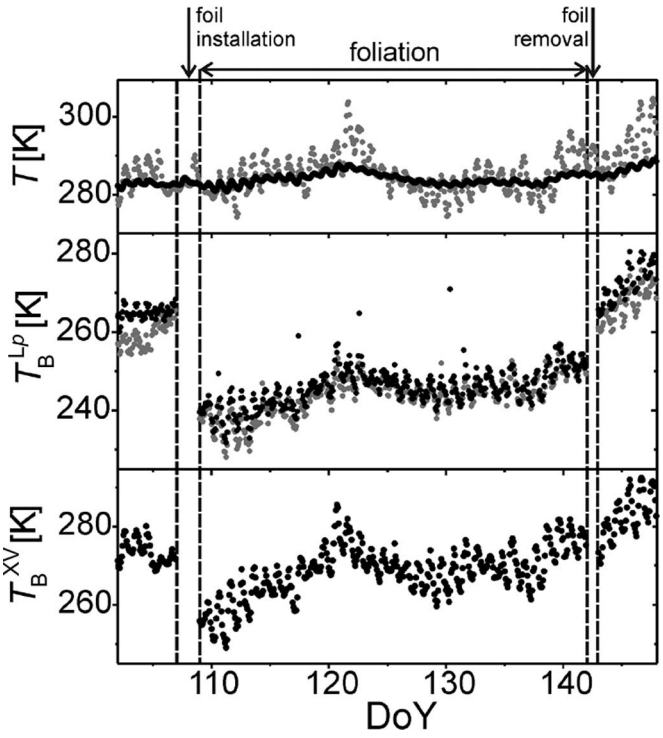

Fig. 4. Foil experiment data set. (a) (black) Forest ground temperature $T_{\rm FG}$ at 5-cm depth and (gray) air temperature $T_{\rm A}$ at 20-m height. (b) L-band brightness temperature $T_{\rm B}^{{\rm L}p}$ at (gray) $p = {\rm H}$ and (black) $p = {\rm V}$. (c) X-band brightness temperature at V-polarization $T_{\rm B}^{\rm XV}$.

B. Foil Experiment

The foil experiment data set taken from Fig. 3, including the measurements performed five days prior to the foil installation and after its removal, is shown in Fig. 4. The foil experiment was started on DoY 109 when the canopy was not yet foliated (relative foliation $= 0$) and ended 34 days later (DoY 142) when the canopy was in its fully foliated state (relative foliation $= 1$). During the two days of foil-installation at the beginning of the experiment and during the removal at the end, no radiometric measurements were taken (data gap between the dotted lines in Fig. 4). The average forest ground and air temperatures during the foil experiment were $\langle T_{\rm FG} \rangle = 284.1$ K $\pm$ 1.6 K and $\langle T_{\rm A} \rangle = 285.7$ K $\pm$ 5.3 K, respectively.

Masking the emission of the forest ground with the highly reflecting foil affected $T_{\rm B}^{{\rm L}p}$ at L-band and $T_{\rm B}^{\rm XV}$ at X-band distinctly different. The measurements at both microwave

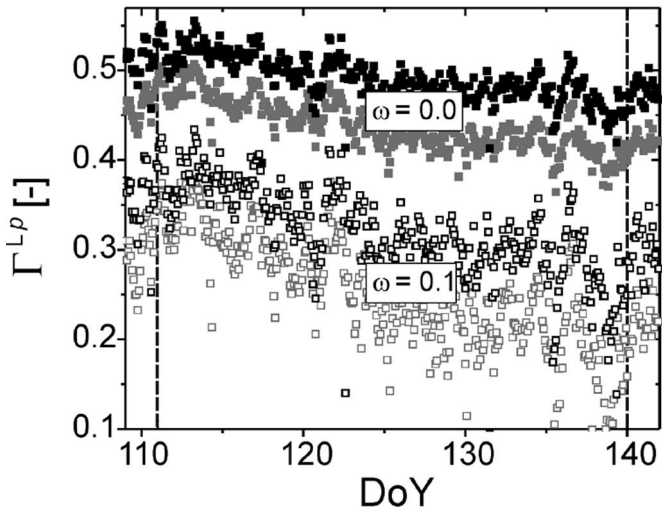

Fig. 5. L-band canopy transmissivities Γ^{Lp} at (gray) $p = \mathrm{H}$ and (black) $p = \mathrm{V}$ during the foil experiment, assuming that (a) (solid) $\omega = 0$ and (b) (hollow) $\omega = 0.1$.

frequencies (1.4 and 11.4 GHz) dropped significantly by virtue of masking the ground below the foliage-free canopy at the beginning of the foil experiment. The corresponding drops of the three-day averages after and before the foil installation were $\Delta T_{\mathrm{B}}^{\mathrm{LH}} \approx -23.6\ \mathrm{K} \pm 1.9\ \mathrm{K}$, $\Delta T_{\mathrm{B}}^{\mathrm{LV}} \approx -24.7\ \mathrm{K} \pm 1.6\ \mathrm{K}$ at L-band, and $\Delta T_{\mathrm{B}}^{\mathrm{XV}} \approx -14.6\ \mathrm{K} \pm 2.0\ \mathrm{K}$ at X-band. Removing the foil in the fully foliated canopy state at the end of the foil experiment increased T_{B}^{Lp} at L-band by comparable absolute values $\Delta T_{\mathrm{B}}^{\mathrm{LH}} \approx +12.5\ \mathrm{K} \pm 2.0\ \mathrm{K}$ and $\Delta T_{\mathrm{B}}^{\mathrm{LV}} \approx +16.1\ \mathrm{K} \pm 2.6\ \mathrm{K}$, whereas the increase at X-band $\Delta T_{\mathrm{B}}^{\mathrm{XV}} \approx +0.8\ \mathrm{K} \pm 4.2\ \mathrm{K}$ was small.

The same order of magnitude of $|\Delta T_{\mathrm{B}}^{Lp}|$ observed for the foliage-free and the foliated state shows that the fraction of the ground emission received at 1.4 GHz is similar at the two extreme canopy states. At 11.4 GHz, the change of the signature due to the removal of the foil below the fully foliated canopy is much less pronounced as compared with the change due to the foil-installation in the absence of leaves. Consequently, at X-band, the ground-emitted radiation contribution [term 1) in (2)] is clearly reduced by the foliage. This confirms that leaves are playing a minor role for radiometric L-band measurements but a key role at X-band.

Knowing the L-band transmissivities $\Gamma^{Lp}(p = \mathrm{H}, \mathrm{V})$ of a specific canopy type is crucial for soil moisture retrieval based on L-band measurements. For this purpose, the L-band transmissivities Γ^{Lp} of the forest were derived from the measurements T_{B}^{Lp} during the foil experiment by applying the radiative transfer model described in Section III. The three different areas $i = 1, 2, 3$ with the local-site parameters $T_{\mathrm{FG},i}$, $T_{\mathrm{V},i}$, $R_{\mathrm{FG},i}$, ω_i, and Γ_i determine the measured T_{B}^{Lp} according to the linear combination (1). The following values of the weights μ_i, which represents the fractional contributions of radiation, are applied: $\mu_1 = 0.5$ for the foil-covered sector with canopy transmissivity $\Gamma_1^{Lp} < 1$; $\mu_2 = 0.07$ for the woodless area with $\Gamma_2^{Lp} = 1$; and $\mu_3 = 0.43$ for the remaining forested area with $\Gamma_3^{Lp} = \Gamma_1^{Lp} < 1$. Equal ground temperatures $T_{\mathrm{FG},1} = T_{\mathrm{FG},2} = T_{\mathrm{FG},3} = T_{\mathrm{FG}}$ within the three areas and equal vegetation temperatures $T_{\mathrm{V},1} = T_{\mathrm{V},3} \approx T_{\mathrm{A}}$ were considered for the forested areas $(i = 1, 3)$. The reflectivity $R_{\mathrm{FG},1}^{p} = 1$ is used at both polarizations $(p = \mathrm{H}, \mathrm{V})$ for the ground masked with the metalized foil assumed as a perfect reflector (Section II-D).

TABLE I
TEMPORALLY AVERAGED TRANSMISSIVITIES $\langle\Gamma^{\mathrm{LH}}\rangle$ AND $\langle\Gamma^{\mathrm{LV}}\rangle$ DERIVED FOR $\omega = 0$ AND $\omega = 0.1$ FROM BRIGHTNESS MEASURED DURING A FOLIAGE-FREE AND A FULLY FOLIATED PERIOD DURING THE FOIL EXPERIMENT

	$\omega = 0$	$\omega = 0.1$	rel. foliation
$\langle\Gamma^{\mathrm{LH}}\rangle$	0.47 ± 0.02	0.31 ± 0.02	0
$\langle\Gamma^{\mathrm{LV}}\rangle$	0.51 ± 0.02	0.36 ± 0.02	(109 ≤ DoY ≤ 111)
$\langle\Gamma^{\mathrm{LH}}\rangle$	0.41 ± 0.01	0.20 ± 0.02	1
$\langle\Gamma^{\mathrm{LV}}\rangle$	0.47 ± 0.02	0.28 ± 0.02	(140 ≤ DoY ≤ 142)

Fig. 5 shows L-band canopy transmissivities Γ^{Lp} derived from the measurements for two values of the effective single-scattering albedo $\omega = \omega_1 = \omega_3 = 0$ (solid) and $\omega = \omega_1 = \omega_3 = 0.1$ (hollow). As a consequence of the assumption $\omega = 0$, the experimentally based transmissivities Γ^{LH} (gray solid) and Γ^{LV} (black solid) include canopy absorption and also scattering if present. Furthermore, the transmissivities $\Gamma^{Lp}(p = \mathrm{H}, \mathrm{V})$ that is derived for $\omega = 0$ (bold) can be compared with the values found in the earlier experiment, in which the microwave emission of the same forest was measured from below the canopy [19].

The decreasing trend of the L-band transmissivities for more developed foliage during the foil experiment (the relative foliation increases from zero to one during the foil experiment) is partly caused by the increasing column density of leaves in the forest crown. Furthermore, the increasing mean daily temperature over the time span of the foliation period (≈5 K) enhances the electrical conductivity losses in the saline water contained in the vegetation [30]. This increases the wave-attenuation coefficients [31] of the tree components, which contributes to the lower canopy transmissivity observed for the fully foliated canopy state. Furthermore, the canopy reveals higher transmissivities for vertically (black solid and hollow) than for horizontally (gray solid and hollow) polarized radiance. However, changing the effective single-scattering albedo ω from 0 to 0.1 significantly reduces the transmissivity values, revealing the considerably high sensitivity of the radiative transfer model with respect to the parameter ω.

Values of temporally averaged transmissivities $\langle\Gamma^{\mathrm{LH}}\rangle$ and $\langle\Gamma^{\mathrm{LV}}\rangle$ observed for $109 \leq \mathrm{DoY} \leq 111$ when the canopy was foliage-free (relative foliation $= 0$) and during a fully foliated period (relative foliation $= 1$) lasting from $140 \leq \mathrm{DoY} \leq 142$ are shown in Table I for $\omega = 0$ and $\omega = 0.1$, respectively. The values $\langle\Gamma^{\mathrm{LH}}\rangle$ and $\langle\Gamma^{\mathrm{LV}}\rangle$ found for $\omega = 0$ are in good agreement with the span of transmissivities 0.41–0.46 observed in [19] for the same canopy and a full-defoliation period. However, not only the absolute values of $\langle\Gamma^{\mathrm{LH}}\rangle$ and $\langle\Gamma^{\mathrm{LV}}\rangle$ are affected by the choice of ω but also their relative changes due to altered canopy foliation state. For $\omega = 0$, $\langle\Gamma^{\mathrm{LH}}\rangle$ and $\langle\Gamma^{\mathrm{LV}}\rangle$ are reduced due to the foliation by ≈13% and ≈8%, whereas the corresponding transmissivities $\langle\Gamma^{\mathrm{LH}}\rangle$ and $\langle\Gamma^{\mathrm{LV}}\rangle$ for $\omega = 0.1$ are reduced by ≈35% and ≈22%. However, the values of the experimentally

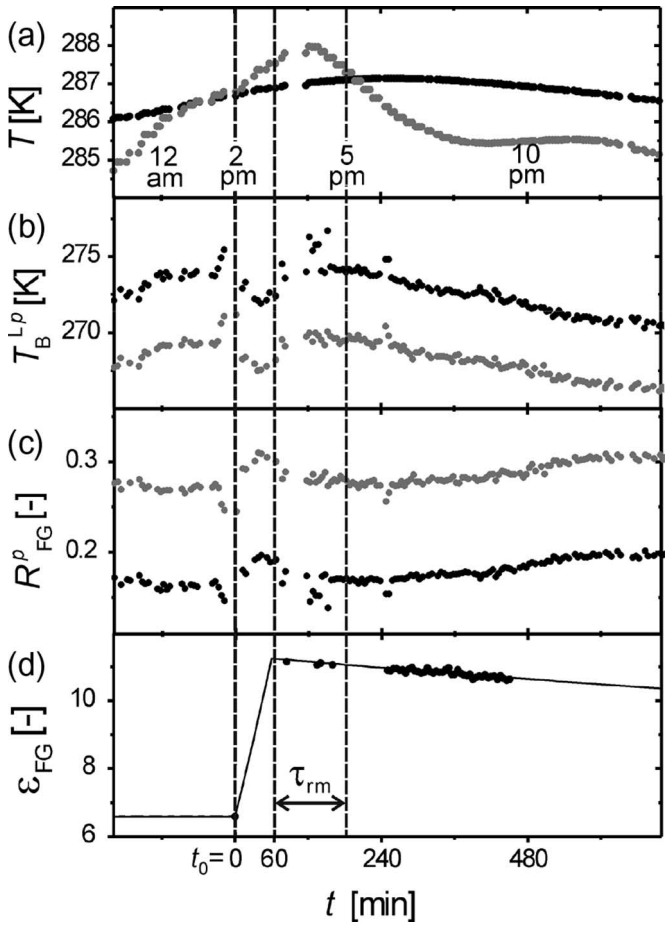

Fig. 6. Irrigation experiment data set. (a) (black) Forest ground and (gray) vegetation temperatures $T_{\rm FG}$ and $T_{\rm V}$. (b) Measured L-band brightness $T_{\rm B}^{Lp}$ for (gray) $p = {\rm H}$ and (black) $p = {\rm V}$. (c) (gray) Forest ground reflectivities $R_{\rm FG}^{\rm H}$ and (black) $R_{\rm FG}^{\rm V}$ derived from $T_{\rm B}^{Lp}$ for $\omega = 0$. (d) TDR-measured permittivities $\varepsilon_{\rm FG}$ 5 cm below (dots) the litter and (line) interpolation.

based transmissivities corroborate the semitransparency of the forest canopy at L-band for any foliation state, which is independent of the assumption made on ω within a reasonable range.

C. Irrigation Experiment

The irrigation of the same area masked in the foil experiment was started at 2 P.M. on DoY 277 (corresponding to $t_0 = 0$ min in Fig. 6). The forest ground was irrigated with a rate of 45.2 mm h^{-1} for 60 min, while wetting the canopy was avoided. On the day of the irrigation experiment, the diurnal mean of the forest ground and vegetation temperature was $\langle T_{\rm FG}\rangle = 286.4\ {\rm K} \pm 0.5\ {\rm K}$ and $\langle T_{\rm V}\rangle = 284.9\ {\rm K} \pm 1.8\ {\rm K}$. Furthermore, the three days following the irrigation were rainless.

In situ forest ground temperatures $T_{\rm FG}$ (black) and vegetation temperatures $T_{\rm V}$ (gray) measured with an infrared RM are shown in Fig. 6(a). Measured L-band brightness $T_{\rm B}^{\rm LH}$ at horizontal polarization (gray) and $T_{\rm B}^{\rm LV}$ at vertical polarization (black) are shown in Fig. 6(b).

Fig. 6(c) shows forest ground reflectivities $R_{\rm FG}^{\rm H}$ (gray) and $R_{\rm FG}^{\rm V}$ (black) deduced from the corresponding measurements $T_{\rm B}^{\rm LH}$ and $T_{\rm B}^{\rm LV}$ using the radiative transfer approach described in Section III. The same weights $\mu_1 = 0.5$, $\mu_2 = 0.07$, and $\mu_3 = 0.43$ of the radiance emitted by the irrigated $(i = 1)$, the woodless $(i = 2)$, and the remaining forested area $(i = 3)$ are considered in the linear combination (1). As the irrigation water was approximately at ambient temperature, uniform temperatures $T_{{\rm FG},1} = T_{{\rm FG},2} = T_{{\rm FG},3} = T_{\rm FG}$ are used for the three ground sections affecting the measured radiance. Equal vegetation temperatures $T_{{\rm V},1} = T_{{\rm V},3} = T_{\rm A}$ and transmissivities $\Gamma^{\rm LH} = \Gamma_1^{\rm LH} = \Gamma_3^{\rm LH} = 0.41$ and $\Gamma^{\rm LV} = \Gamma_1^{\rm LV} = \Gamma_3^{\rm LV} = 0.47$ deduced in the previous foil experiment (Section IV-B) are considered for the forested areas. The latter two assumptions are reasonable, as wetting the fully foliated forest canopy was avoided in the irrigation experiment. Furthermore, the effective single-scattering albedo $\omega = \omega_1 = \omega_3 = 0$ of the forest canopy is assumed for the computation of the shown reflectivities.

Fig. 6(d) shows forest ground permittivities $\varepsilon_{\rm FG}$ measured *in situ* with TDR probes installed 5 cm below the litter layer within the irrigated area. The solid line is an interpolation corresponding to the TDR measured data (dots). The data measured subsequent to the irrigation phase $(t \geq t_0 + 60\ {\rm min})$ are interpolated using a decaying exponential comprising the characteristic residence time $\tau_{5\,{\rm cm}}$ as a fitting parameter in the exponent. The determined residence time $\tau_{5\,{\rm cm}} \approx 3326$ min expresses the time needed to reduce the moisture that is 5 cm below the surface to similar values, as observed immediately before sprinkling.

As the result of the irrigation, a depression in the measured $T_{\rm B}^{Lp}$ can be observed during $t_0 \leq t \leq t_0 + 60$ min corresponding to the time of irrigation [Fig. 6(b)]. The brightness temperatures at both polarizations are decreased by approximately 2 K. After the irrigation, $T_{\rm B}^{Lp}$ increased immediately, approaching the typical diurnal trend within the following period $\tau_{\rm rm} \approx 120$ min.

The observed depression in $T_{\rm B}^{Lp}$ during the time of irrigation can either be caused by cooling of the scene due to water evaporation (latent heat) or by increased forest ground reflectivity $R_{\rm FG}^{p}$ as the result of increased permittivity $\varepsilon_{\rm FG}$ of the watered forest ground. However, the effect on the signature caused by cooling the ground is expected to be reduced in the time series of the ground reflectivities $R_{\rm FG}^{p}$, shown in Fig. 6(c). As shown, the reflectivities $R_{\rm FG}^{p}$ are distinctly increased for the period $t_0 \leq t \leq t_0 + 60$ min and, thus, are clearly positively correlated with irrigation. This indicates that the observed depression in $T_{\rm B}^{Lp}$ during the irrigation is predominantly caused by the increased ground-surface permittivity.

The reflectivities $R_{\rm FG}^{p}$ for both polarizations $(p = {\rm H}, {\rm V})$ decrease during the period $\tau_{\rm rm} \approx 120$ min subsequent to the irrigation phase to similar values, as observed immediately before irrigation. The period $\tau_{\rm rm}$, while the L-band signatures are affected by the irrigation, is clearly smaller than the characteristic residence time $\tau_{5\,{\rm cm}} \approx 3326$ min of moisture that is 5 cm below the litter layer. Considering a relatively fast drainage time of the irrigated water through the litter layer, which is of the same order as $\tau_{\rm rm}$, suggests the following hypothesis.

The observed L-band signature caused by increased forest ground moisture is mainly the result of the increased

near-surface moisture. The radiometrically relevant part of a forest ground might even be exclusively restricted to the litter layer. This means that L-band brightness temperatures measured above forested sites are potentially carrying information on the litter moisture, whereas the water content of the underlying soil might be totally shielded.

V. Conclusion

The FOSMEX was a one-year-long microwave campaign monitoring the emission at L- and at X-band from a platform above a deciduous forest. A zeroth-order radiative transfer approach was applied for the interpretation of the measured brightness temperatures in terms of canopy transmissivities associated with the canopy foliation state and forest ground reflectivities related with forest ground moisture.

Canopy transmissivities have been investigated in the foil experiment by dint of a metalized foil installed for masking a considerable fraction of the forest ground emission. For the foliage-free canopy, the reflecting foil reduced the L-band brightness by $\approx$24 K and the corresponding effect caused by the removal of the foil in the fully foliated canopy state caused an increase of $\approx$14 K. Depending on the assumption made on the single-scattering albedo ω of the canopy, the transmissivities were on the order of 0.47 for $\omega = 0$ and 0.29 for $\omega = 0.1$. The corresponding relative impacts on the canopy transmissivities caused by the foliation state were estimated to be 10.5% (for $\omega = 0$) and 28.5% (for $\omega = 0.1$), respectively.

The results reveal the semitransparency of the canopy at L-band at any foliation state, indicating that the detection of the forest ground radiation is generally possible. However, the sensitivity of the measured brightness with respect to moisture changes in the forest ground is substantially reduced by the presence of the crown canopy for all foliation states.

The intense irrigation of the forest ground performed in the irrigation experiment produced a measurable signature in the L-band brightness. The signature is identified to be caused by the increased permittivity of the near-surface forest ground associated with the deployed water. From the observed fast fading of the signature after the irrigation phase, it is apparent that L-band brightness temperatures measured above forested sites are potentially carrying information on the litter moisture, while inferring the water content of the underlying soil might be very critical.

The observed obscuring effect of litter on the radiance emitted from below and the fast drainage time of water through the litter layer show that microwave signatures have to be measured with high temporal resolution for identifying an individual precipitation. Moreover, highly accurate instruments are required because the microwave signature caused by changes in the forest ground water content is generally little, and even short-lived, if litter is present.

In the light of these conclusions, we note that the envisaged accuracy of soil moisture expected from the SMOS mission (4%) might be critical for areas comprising a significant amount of litter. However, forest-emitted L-band radiation provides information about the litter moisture that might be related with the subjacent soil water content if adequate hydrological models are used. Therefore, studies regarding the water exchange between litter and soil are needed and expected to improve the interpretation of L-band signatures emitted from forests.

Acknowledgment

The authors would like to thank Dr. A. Knaps of the Research Centre Jülich for providing the meteorological data, R.-U. Limbach for taking photographs, and O. Muggli of the Alcan Packaging Services, Ldt., Neuhausen, Switzerland, for sponsoring the metalized foil. The setting of instruments has been supported by Hannes Wydler and Jörg Leuenberger from the Institute of Terrestrial Ecosystems, ETH Zurich.

References

[1] E. A. Sharkov, *Passive Microwave Remote Sensing of the Earth: Physical Foundations*. Berlin, Germany: Springer-Verlag, 2003.

[2] T. Schmugge, "Applications of passive microwave observations of surface soil moisture," *J. Hydrol.*, vol. 212/213, pp. 188–197, Dec. 1998.

[3] T. J. Jackson, D. M. Le Vine, A. Y. Hsu, A. Oldak, P. J. Starks, C. T. Swift, J. D. Isham, and M. Haken, "Soil moisture mapping at regional scales using microwave radiometry: The Southern Great Plains Hydrology Experiment," *IEEE Trans. Geosci. Remote Sens.*, vol. 37, no. 5, pp. 2136–2151, Sep. 1999.

[4] E. G. Njoku, T. J. Jackson, V. Lakshmi, T. K. Chan, and S. V. Nghiem, "Soil moisture retrieval from AMSR-E," *IEEE Trans. Geosci. Remote Sens.*, vol. 41, no. 2, pp. 215–229, Feb. 2003.

[5] Y. Kerr, P. Waldteufel, J.-P. Wigneron, J.-M. Martinuzzi, J. Font, and M. Berger, "Soil moisture retrieval from space: The Soil Moisture and Ocean Salinity (SMOS) mission," *IEEE Trans. Geosci. Remote Sens.*, vol. 39, no. 8, pp. 1729–1735, Aug. 2001.

[6] W. Burke, T. Schmugge, and J. Paris, "Comparison of 2.8- and 21-cm microwave radiometer observations over soils with emission model calculations," *J. Geophys. Res.*, vol. 84, no. C1, pp. 287–294, Jan. 1979.

[7] T. J. Jackson and T. Schmugge, "Passive microwave remote sensing system for soil moisture: Some supporting research," *IEEE Trans. Geosci. Remote Sens.*, vol. 27, no. 2, pp. 225–235, Mar. 1989.

[8] R. H. Lang, C. Utku, P. de Matthaeis, N. Chauhan, and D. M. Le Vine, "ESTAR and model brightness temperatures over forests: Effect of soil moisture," in *Proc. IGARSS*, Sydney, Australia, 2001, pp. 1300–1302.

[9] M. A. Karam, A. K. Fung, R. H. Lang, and N. S. Chauhan, "A microwave scattering model for layered vegetation," *IEEE Trans. Geosci. Remote Sens.*, vol. 30, no. 4, pp. 767–784, Jul. 1992.

[10] P. Ferrazzoli and L. Guerriero, "Passive microwave remote sensing of forests: A model investigation," *IEEE Trans. Geosci. Remote Sens.*, vol. 34, no. 2, pp. 433–443, Mar. 1996.

[11] A. Della Vecchia, K. Saleh, P. Ferrazzoli, L. Guerriero, and J.-P. Wigneron, "Simulating L-band emission of coniferous forests using a discrete model and a detailed geometrical representation," *IEEE Geosci. Remote Sens. Lett.*, vol. 3, no. 3, pp. 364–368, Jul. 2006.

[12] P. Ferrazzoli, L. Guerriero, and J.-P. Wigneron, "Simulating L-band emission of forests in view of future satellite applications," *IEEE Trans. Geosci. Remote Sens.*, vol. 40, no. 12, pp. 2700–2708, Dec. 2002.

[13] K. Saleh, A. Porté, D. Guyon, P. Ferrazzoli, and J. P. Wigneron, "A forest geometric description of a maritime pine forest suitable for discrete microwave models," *IEEE Trans. Geosci. Remote Sens.*, vol. 43, no. 9, pp. 2024–2035, Sep. 2005.

[14] M. T. Hallikainen, P. A. Jolma, and J. M. Hyyppa, "Satellite microwave radiometry of forest and surface types in Finland," *IEEE Trans. Geosci. Remote Sens.*, vol. 26, no. 5, pp. 622–628, Sep. 1988.

[15] G. Macelloni, S. Paloscia, P. Pampaloni, and R. Ruisi, "Airborne multifrequency L- to Ka-band radiometric measurements over forests," *IEEE Trans. Geosci. Remote Sens.*, vol. 39, no. 11, pp. 2507–2513, Nov. 2001.

[16] J. P. Grant, J.-P. Wigneron, A. A. Van de Griend, A. Kruszewsky, S. Schmidl Søbjærg, and N. Skou, "A field experiment on microwave forest radiometry: L-band signal behaviour for varying conditions of surface wetness," *Remote Sens. Environ.*, vol. 109, no. 1, pp. 10–19, Jul. 2007.

[17] C. Mätzler, "Microwave transmissivity of a forest canopy: Experiments made with a beech," *Remote Sens. Environ.*, vol. 48, no. 2, pp. 172–180, 1994.

[18] P. Pampaloni, "Microwave radiometry of forests," *Waves Random Media*, vol. 14, no. 2, pp. S275–S298, Apr. 2004.
[19] M. Guglielmetti, M. Schwank, C. Mätzler, C. Oberdörster, J. Vanderborght, and H. Flühler, "Measured microwave radiative transfer properties of a deciduous forest canopy," *Remote Sens. Environ.*, vol. 109, no. 4, pp. 523–532, 2007.
[20] G. C. Topp, J. L. Davis, and A. P. Annan, "Electromagnetic determination of soil water content: Measurements in coaxial transmission lines," *Water Resour. Res.*, vol. 16, no. 3, pp. 574–582, 1980.
[21] J.-P. Wigneron, Y. Kerr, P. Waldteufel, K. Saleh, M. J. Escorihuela, P. Richaume, P. Ferrazzoli, P. de Rosnay, R. Gurney, J. C. Calvet, J. P. Grant, M. Guglielmetti, B. Hornbuckle, C. Mätzler, T. Pellarin, and M. Schwank, "L-band microwave emission of the biosphere (L-MEB) model: Description and calibration against experimental data sets over crop fields," *Remote Sens. Environ.*, vol. 107, no. 4, pp. 639–655, Apr. 2007.
[22] C. Mätzler, D. Weber, M. Wüthrich, K. Schneeberger, C. Stamm, and H. Flühler, "ELBARA, the ETH L-band radiometer for soil moisture research," in *Proc. Int. Geosci. Remote Sens. Symp.*, Toulouse, France, 2003, pp. 3058–3060.
[23] *Handbook of the MORA 11.4 GHz Radiometer*, Inst. Appl. Phys., Bern, Switzerland, 1991.
[24] H. M. Pickett, J. C. Hardy, and J. Farhoomand, "Characterization of a dual-mode horn for submillimeter wavelengths," *IEEE Trans. Microw. Theory Tech.*, vol. MTT-32, no. 8, pp. 936–937, Aug. 1984.
[25] F. Ulaby, R. Moore, and A. Fung, *Microwave Remote Sensing Active and Passive*, vol. 1. Reading, MA: Addison-Wesley, 1981.
[26] J. C. Jenkins, D. C. Chojnacky, L. S. Heath, and R. A. Birdsey, "National-scale biomass estimators for united states tree species," *For. Sci.*, vol. 49, no. 1, pp. 12–35, 2003.
[27] Y. Kerr and E. G. Njoku, "A semiempirical model for interpreting microwave emission from semiarid land surfaces as seen from space," *IEEE Trans. Geosci. Remote Sens.*, vol. 28, no. 3, pp. 384–393, May 1990.
[28] C. Mätzler, P. W. Rosenkranz, A. Battaglia, and J.-P. Wigneron, *Thermal Microwave Radiation: Applications for Remote Sensing*, ser. IET Electromagnetic Waves Series. London, U.K.: IET, 2006.
[29] S. Paloscia and P. Pampaloni, "Microwave polarization index for monitoring vegetation growth," *IEEE Trans. Geosci. Remote Sens.*, vol. 26, no. 5, pp. 617–621, Sep. 1988.
[30] T. Meissner and F. J. Wentz, "The complex dielectric constant of pure and sea water from microwave satellite observations," *IEEE Trans. Geosci. Remote Sens.*, vol. 42, no. 9, pp. 1836–1849, Sep. 2004.
[31] J. C. Santamarina and K. A. Klein, "Part 4: Electromagnetic waves and soils," in *Soils and Waves*. Hoboken, NJ: Wiley, 2001, pp. 318–321.

Massimo Guglielmetti received the M.S. and Ph.D. degrees in environmental sciences from the Swiss Federal Institute of Technology Zürich, Zürich, Switzerland, in 2003 and 2007, respectively. The topic of his Master thesis in soil physics was "Quantitative description of tracer distribution in heterogenic sands." The topic of his Ph.D. thesis was inferring forest soil water content with microwave radiometry.

Mike Schwank received the Ph.D. degree in physics from the Swiss Federal Institute of Technology Zürich, Zürich, Switzerland, in 1999. The topic of his Ph.D. thesis was "nano-lithography using a high-pressure scanning–tunneling microscope."

In the following three years, he gained experience in the industrial environment where he worked as a Research and Development Engineer in the field of microoptics. Since 2003, he has been working in the research field of microwave remote sensing applied to soil moisture detection. He is currently working as a Senior Research Assistant with the Swiss Federal Institute for Forest, Snow and Landscape Research (WSL). His research involves practical and theoretical aspects of microwave radiometry. In addition to his research at the WSL he works for the company Gamma Remote Sensing, Gümligen, Switzerland, where he is involved in the production of microwave radiometers to be deployed for ground-based soil moisture and ocean salinity calibration/validation purposes.

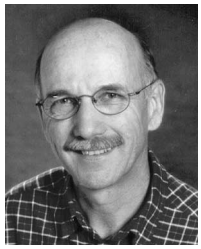

Christian Mätzler (M'96–SM'03) received the M.Sc. degree in physics with subsidiaries in mathematics and geography and the Ph.D. degree with a Doctoral thesis in solar radio astronomy from the University of Bern, Bern, Switzerland, in 1970 and 1974, respectively.

He made postdoctoral studies with the NASA Goddard Space Flight Center, Greenbelt, MD, and with the Swiss Federal Institute of Technology Zürich, Zürich, Switzerland. He is currently a Titularprofessor of applied physics and remote sensing, leading the Radiometry for Environmental Monitoring Project Group, with the Institute of Applied Physics, University of Bern. His experimental studies have concentrated on surface-based microwave (1–100 GHz) signatures for active and passive microwave remote sensing of snow, ice, soil, vegetation, and atmosphere, including precipitation, clouds, and the boundary layer, and on the development of methods for dielectric measurements of these media, with complementary work at optical wavelengths. He is interested in meteorological applications of remote sensing and in improvements of the physical understanding of the processes involved. Based on the experimental work of his group, he has developed and tested microwave (1–100 GHz) propagation, transmission, emission, scattering, and dielectric models of snowpacks and of the atmosphere.

Dr. Mätzler is a member of the International Glaciological Society.

Christoph Oberdörster received the M.S. degree in agricultural sciences from the University of Bonn, Bonn, Germany, in 2004. His M.S. thesis was the "Verification of the Mualem-Friedman model in soil columns under transient conditions by means of TDR." He is currently working toward the Ph.D. degree with the Agrosphere Institute, Institute of Chemistry and Dynamics of the Geosphere (ICG-4), Forschungszentrum Jülich GmbH, Jülich, Germany. His Ph.D. research is focused on the measurement and simulation of water fluxes in a forest stand.

Jan Vanderborght received the B.Eng. degree in agricultural engineering and the Ph.D. degree in applied biological sciences from the Katholieke Universiteit Leuven (KUL), Leuven, Belgium, in 1993 and 1997, respectively.

He is currently a Senior Scientist with the Agrosphere Institute, Institute of Chemistry and Dynamics of the Geosphere (ICG-4), Forschungszentrum Jülich GmbH, Jülich, Germany, leading the Transport in Soils and Groundwater Research Group. Since 2005, he has also been a part-time Professor of soil physics with the Department of Land Management and Economy, KUL. His research interests include the modeling and monitoring of flow and transport processes in heterogeneous soil–plant systems using tomographic geophysical methods.

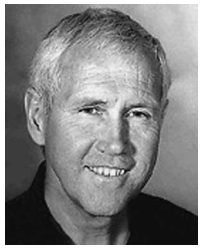

Hannes Flühler received the Ph.D. degree from the Swiss Federal Institute of Technology (ETH) Zürich, Zürich, Switzerland, in 1972.

He did his postgraduate studies in soil physics with ETH Zurich in 1973 and at the University of California at Riverside, Riverside, from 1974 to 1976. From 1977 to 1980, he led the Biophysics Group with the Federal Institute for Forestry Research, where from 1980 to 1983, he chaired the Vegetation and Soil Section. From 1983 to his retirement in 2007, he was a Professor of soil physics with ETH Zurich. His research is focussed on transport processes in soil, specifically in methodology, but also in relation to environmental applications.